Chapter 9
Simulations and Analysis of BeiDou Navigation Satellite System (BDS)-Relectometry Delay-Doppler Maps for Vegetation

Xuerui Wu and Shuanggen Jin

Abstract Global Positioning System-Reflectometry (GPS-R) is a new promising technique, which uses the reflected signals of the GPS constellation to remotely sense the geophysical parameters of the ocean and land surface. Some initial results were obtained from GPS-R in ocean surface characteristics and soil moisture, while, vegetation sensing is paid attention recently. With the development of Chinese independent Beidou Satellite Navigation System (BDS), it will play a key role in positioning, navigation and timing as well as potential applications of BDS-Reflectometry (BDS-R), e.g. vegetation monitoring using the Delay-Doppler Map (DDM) of BDS-R. Therefore, it is extremely necessary to simulate the vegetation BDS-R DDM maps. Z–V model is a commonly used GPS-R scattering model and its applications include the sea wind, oil slick and soil moisture. In this paper, it is the first time for vegetation DDM simulations from BDS-R, while the vegetation scattering properties are simulated using the modified Bi-mimics model, which can be used to calculate any transmit and receive polarization combinations, assuming that the received power is coming from the first Fresnel zone. The theoretical simulations of DDM are helpful for the further BDS-R vegetation parameters retrieval, and some discussions and analysis are further given.

Keywords BDS-R · Vegetation · Z–V · Bi-mimics · DDM

X. Wu (✉) · S. Jin
Shanghai Astronomical Observatory, Chinese Academy of Sciences,
Shanghai 200030, China
e-mail: xrwu@shao.ac.cn

S. Jin
e-mail: sgjin@shao.ac.cn

X. Wu
Department of Environment Resources and Management, Chifeng University,
Chifeng, Inner, Mongolia 024000, China

J. Sun et al. (eds.), *China Satellite Navigation Conference (CSNC) 2014 Proceedings: Volume I*, Lecture Notes in Electrical Engineering 303,
DOI: 10.1007/978-3-642-54737-9_9,

9.1 Introduction

GNSS-Reflectometry (GNSS-R) was first proposed by Martin-Neira in the early 1990s for altimetry measurement [1]. In the following years, its applications were extended from mesoscale ocean [2] to land surface [3] as well as snow/ice remote sensing [4, 5]. As for the land scenario, soil moisture and vegetation characteristics study are the main purposes [3]. With the development of Chinese independent BeiDou Navigation Satellite System (BDS), it will play a key role in positioning, navigation and timing as well as potential applications of BDS-Reflectometry (BDS-R), e.g. vegetation monitoring using the BDS-R DDM maps. Z–V scattering model was first developed by Zavorotny and Voronovich in 2000 for ocean wind remote sensing [2], which is commonly used for DDM simulations. An efficient algorithm of ZV model was proposed in 2009 for the resource computation consideration (both time and memory) [6]. At present, GNSS-R delay-doppler maps simulations commonly use the Z–V model, such as DDM simulations of ocean wind and oil slick [7]. As for land part, the reflected signal waveform was initially modeled by Masters [8] using Z–V model. KA-GO model was used for soil scattering calculations. However, the Delay Doppler Map simulations of vegetation analysis are still not yet.

This paper focuses on the vegetation DDM simulations using modified Z–V model from BDS-R. The Bi-mimics model [9] is used for vegetation scattering calculations and then Z–V model is used for DDM waveform simulations [2]. In Sect. 9.2, the Bi-mimics model is described and the Z-V model is presented in Sect. 9.3. Initial simulations results are given in Sect. 9.4. And finally, some discussions and conclusions are given in Sect. 9.5.

9.2 Bi-mimics Model

As for GNSS-R remote sensing, GNSS constellations are the source of transmitted signals and the corresponding receiver collects the reflected signals, which form a typical bistatic/multi-static radar working mode. The bistatic scattering model Bi-mimics [9] is adopted in our work to calculate vegetation scattering characteristics.

9.2.1 Basic Formulations

The Bi-mimics model is a bistatic forest scattering model [9], which is based on the first order radiative transfer MIMICS (Michigan Microwave Canopy Scattering) model [10]. The canopy structure is modeled as crown layer and trunk layer over a dielectric ground surface. Assuming that I_i and I_s are the incident intensity and scattering intensity, respectively and (θ_i, φ_i) and (θ_s, φ_s) are the corresponding

incident and scattering angles, the first-order fully polarimetric transformation matrix T is used to relate I_i and I_s.

$$I_s(\theta_s, \varphi_s) = T(\theta_s, \varphi_s) I_i(\theta_i, \varphi_i) \tag{9.1}$$

T is given in terms of the extinction and phase matrices, which are calculated by the average modified Mueller matrices. Note that there are eight scattering mechanisms in this model. Contributions from layers of crown, trunk and ground amount to the final scattering.

9.2.2 Wave Synthesis

As for GNSS-R remote sensing, the transmitted signals are the Right-Hand Circular Polarization (RHCP) polarization, which is different from the original linear polarizations used in conventional microwave techniques. Therefore, we need to make it possible for the circular polarization calculation using Bi-mimics model [9–11].

As we know, the Bi-mimics model is a fully polarimetric model. The bistatic scattering cross section for any combinations of transmit and receive polarizations can be achieved by Eq. (9.2)

$$\sigma_{rt}(\psi_r, \chi_r, \psi_t, \chi_t) = 4\pi \tilde{Y}_m^r M Y_m^t \tag{9.2}$$

where M is the Muller matrix by a 4 × 4 real matrix, see Eq. (9.3–9.5), $\tilde{R}$ is the transpose of R, as shown in Eq. (9.5), and Y_m^t and Y_m^r are the modified Stokes vectors in Eq. (9.6).

$$M = \tilde{R}^{-1} W R^{-1} \tag{9.3}$$

$$W = \begin{bmatrix} S_{vv}S_{vv}^* & S_{vh}S_{vh}^* & S_{vv}S_{vh}^* & S_{vh}S_{vv}^* \\ S_{hv}S_{hv}^* & S_{hh}S_{hh}^* & S_{hv}S_{hh}^* & S_{hh}S_{hv}^* \\ S_{vv}S_{hv}^* & S_{vh}S_{hh}^* & S_{vv}S_{hh}^* & S_{vh}S_{hv}^* \\ S_{hv}S_{vv}^* & S_{hh}S_{vh}^* & S_{hv}S_{vh}^* & S_{hh}S_{vv}^* \end{bmatrix} \tag{9.4}$$

$$R = \begin{bmatrix} 1 & 1 & 0 & 0 \\ 1 & -1 & 0 & 0 \\ 0 & 0 & 1 & 1 \\ 0 & 0 & -j & j \end{bmatrix} \tag{9.5}$$

$$Y_m^t = \begin{bmatrix} \frac{1}{2}(1+\cos 2\psi_t \cos 2\chi_t) \\ \frac{1}{2}(1-\cos 2\psi_t \cos 2\chi_t) \\ \sin 2\psi_t \cos 2\chi_t \\ \sin 2\chi_t \end{bmatrix} \quad Y_m^r = \begin{bmatrix} \frac{1}{2}(1+\cos 2\psi_r \cos 2\chi_r) \\ \frac{1}{2}(1-\cos 2\psi_r \cos 2\chi_r) \\ \sin 2\psi_r \cos 2\chi_r \\ \sin 2\chi_r \end{bmatrix} \tag{9.6}$$

where (ψ_r, χ_r) are the orientation and ellipcity angles for transmitted signals and (ψ_t, χ_t) are the corresponding angles for the received signals.

Using the above mentioned wave synthesis technique, the scattering coefficients of any combination polarization can be achieved. In this paper, RR and RV polarization of Aspen [10] is selected, and only two single scatters are needed, branch and trunk.

9.3 Z–V Model

9.3.1 Scattering Geometry

To simplify our analysis and focus on the problem itself, we do not care about the curvature of the Earth. We should define the coordinate system at first. The specular point is at the origin of the system, Z-axis is vertical and the x-y plane is the plane tangent to the surface. The scattering geometry is depicted in Fig. 9.1. The h0 and h are the height of the transmitter and receiver, and γ is the elevation angle.

$\vec{R}_t$ is the position from transmitter to the origin of the system. $\vec{R}_r$ is the position from the receiver to the origin of the system. $\vec{R}_{sp}$ is the position of the specular point.

$$\vec{R}_t = \begin{bmatrix} \vec{i} & \vec{j} & \vec{k} \end{bmatrix} \begin{bmatrix} 0 \\ h_0 \cot\gamma \\ h_0 \end{bmatrix} \quad \vec{R}_r = \begin{bmatrix} \vec{i} & \vec{j} & \vec{k} \end{bmatrix} \begin{bmatrix} 0 \\ -h \cot\gamma \\ h \end{bmatrix} \quad \vec{R}_{sp} = \begin{bmatrix} \vec{i} & \vec{j} & \vec{k} \end{bmatrix} \begin{bmatrix} 0 \\ 0 \\ 0 \end{bmatrix} \tag{9.7}$$

$R_{0,sp}$ is the distance from transmitter to the specular point. R_{sp} is the distance from the receiver to the specular point.

$$R_{0,sp} = \sqrt{(h_0 \cot\gamma)^2 + h_0^2}, \quad R_{sp} = \sqrt{(h \cot\gamma)^2 + h^2} \tag{9.8}$$

9.3.2 Z–V Model

The final form of GNSS-R scattering model is shown in the Eq. (9.9). Essentially, it's the integral form of bistatic radar equation.

Fig. 9.1 Scattering geometry

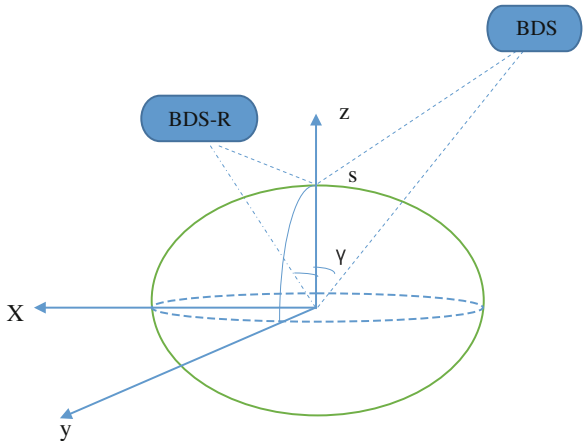

The scattered power is determined by four zones. The first one is the equi-range zones or Fresnel Zone decided by the triangular function, it is a series of elliptical areas with the transmitter and receiver as foci, their interaction with the ocean surface thus forming equi-range. The second one is the Doppler zone determined by the correlation function S, it is a series of hyperbolic curves. The reflected surface roughness is related to the glistening zone. And the function of G is used to define the effective coverage area of the antenna. The final integral region is defined by the above four functions.

As for the ocean part, its roughness scale is comparable or larger than the incoming wavelength, there is a large glistening zone and it may extend several delays away from the specular point. Therefore, not only the quasi-specular scattering component contribute to the aggregate GPS scattering signals, but also the diffractions scattering or Bragg scattering exerts an important role for the finally received waveform.

However, as for land scenario, its roughness scales are well below L-band wavelength, and it does not own a glistening zone, therefore only the coherent part of specular directions are contributed to the overall received GNSS reflected signals. The final contribution to the received GPS signals were thought to come from the first Fresnel Zone. That is to say, only the first elliptical contributed to the final received signals. Here we thought vegetation is uniform in this elliptical area, we use a specular scattering coefficient to represent the total scattering coefficients. And it is calculated by the modified Bi-mimics model.

The final form of Z–V model [2] is shown in Eq. (9.9).

$$\left\langle |Y(\tau)|^2 \right\rangle = T_i^2 \int \frac{D^2(\vec{\rho})\Lambda^2[\tau - (R_0 + R)/c]}{4\pi R_0^2 R^2} \times |S[f_D(\vec{\rho}) - f_c]|^2 \sigma_0(\vec{\rho}) d^2\rho \quad (9.9)$$

where T_i is coherence time. As for the low gain antenna, D is assumed to be unity here (D = 1). Ambiguity function χ is approximated by the triangular function Λ

(also known as pseudorandom code autocorrelation function) and the Doppler filter function S,

$$\chi(\delta\tau, \delta f) = \Lambda(\delta\tau)S(\delta f) \tag{9.10}$$

where $\delta\tau = \tau - \left[R_{0,sp} + R_{sp}\right]/c$ and δf is the Doppler shift due to motions of transmitter and receiver. As for ocean part, intrinsic motions of the surface should be considered. But as for land surface, it is static and there is no need for the consideration of intrinsic surface motions.

$$\delta f(t_0 + \tau) = f_D(t_0 + \tau) = \left[\vec{V}_t \cdot \vec{m} - \vec{V}_r \cdot \vec{n}\right]/\lambda \tag{9.11}$$

where $\vec{V}_t$ and $\vec{V}_r$ are the velocities of transmitter and receiver, $\vec{m}$ and $\vec{n}$ are the unit vectors the incident wave and scattered wave. As for the Doppler shift function S, it is depicted in the following equation,

$$s(\Delta f) = \chi(0, \Delta f) = \frac{\sin(\pi\Delta f T_i)}{(\pi\Delta f T_i)} e^{-\pi i \Delta f T_i} \tag{9.12}$$

As for the triangular function, when $\Delta\tau$ is equal or smaller than τ_c, it is approximated as $1 - \frac{|\Delta\tau|}{\tau_c}$, otherwise, it is 0.

$$\Lambda(\Delta\tau) = \chi(\Delta\tau, 0) \approx \begin{cases} 1 - \frac{|\Delta\tau|}{\tau_c}, & |\Delta\tau| \le \tau_c \\ 0, & |\Delta\tau| > \tau_c \end{cases} \tag{9.13}$$

We have pointed out that only the scattered signals coming from the first Fresnel Zone contribute to the final GNSS-R scattering power. Therefore, we need not integrate as in the ocean part. And the final form of Z–V model is simplified.

9.4 Simulations and Results

This section will give the simulations specular scattering of Aspen and its DDM. As for airborne GNSS-R flight, the commonly incident angles vary between 5° and 45°. Theoretical and experimental data have proven that V polarization is more compatible for the reflected signals. Azimuth angle effects is not considered here and $\varphi_s = \varphi_i = 0°$. That is to say, the incident wave and the scattered wave are in the same plane.

We can see from the simulations (Fig. 9.2) that the co-polarization RR is larger than the cross one RV. For the incident angles vary from 5° to 45°, the differences of scattering coefficient are about 4.4–7.2 dB.

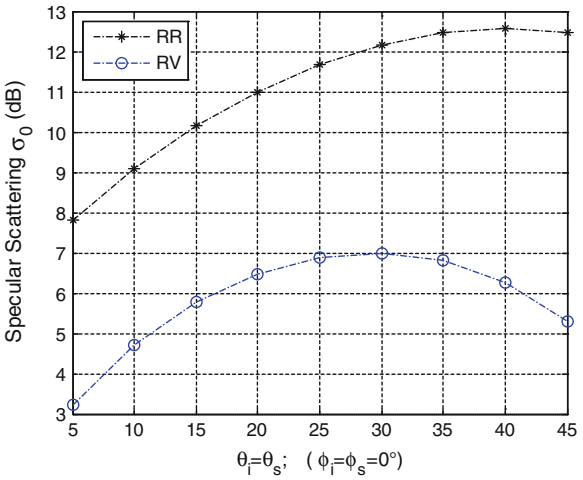

Fig. 9.2 Specular scattering versus specular incident angles

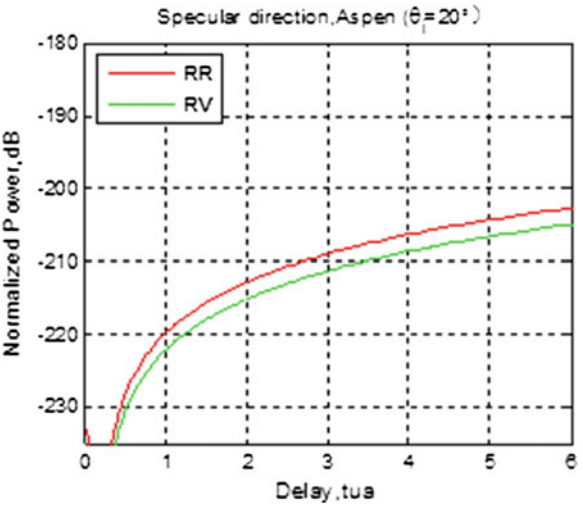

Fig. 9.3 Normalized power versus time delay $\theta_i = 20°$

The Figs. 9.3, 9.4 give the DDM of Aspen, where $\theta_i = 20°$ (Fig. 9.3) and $\theta_i = 40°$ (Fig. 4). The normalized power at $\theta_i = 40°$ is larger than $\theta_i = 20°$ and the power at RR pol is larger than at the RL pol. As the delay increases, the power increases. But it increase sharply when delay is small (0–1). The magnitude of the power is comparable to the theoretical simulations, which use the basic bistatic radar equation [12].

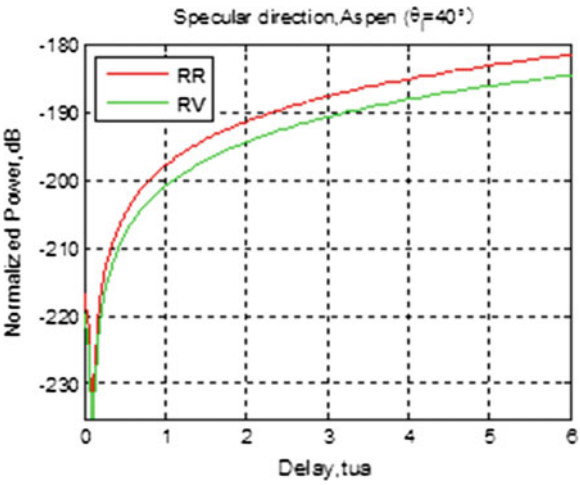

Fig. 9.4 Normalized power versus time delay ($\theta_i = 40°$)

9.5 Conclusions

GNSS-R is a new promising remote sensing technique, particularly in land surface applications due to its L-band working frequency, which is a better bandwidth for penetration and suitable of soil moisture and vegetation monitoring. In this paper, the DDM is the first simulated using the Z–V model for the land surface, here vegetation as an example. The Bi-mimics is used for the calculations of vegetation scattering coefficient. DDM of RR and RV pol at the specular directions are simulated. The results show that DDM forms in the land surface are very different from the ocean surface, whose glistening zone is much larger than the land surface.

Acknowledgments The work is supported by the Natural Science Foundation of the Inner Mongolia Autonomous Region (Grant No. 2013MS0602), Main Direction Project of Chinese Academy of Sciences (Grant No.KJCX2-EW-T03) and National Natural Science Foundation of China (NSFC) Project (Grant No. 11173050 and 11373059).

References

1. Martin-Neira M (1993) A passive reflectometry and interferometry system (PARIS): application to ocean altimetry. ESA J 17:331–355
2. Zavorotnyy V, Voronovich AG (2000) Scattering of GPS signals from the ocean with wind remote sensing application. IEEE Trans Geosci Remote Sens 38(3):951–964
3. Rodriguez-Alvarez N, Camps A, Vall-llossera M et al (2011) Land geophysical parameters retrieval using the interference pattern GNSS-R technique. IEEE Trans Geosci Remote Sens 49(1):71–84. doi:10.1109/TGRS.2010.2049023
4. Cardellach E, Fabra F, Nogués-Correig O, Vall-llossera M et al (2011) GNSS-R ground-based and airborne campaigns for ocean, land, ice, and snow techniques: application to the GOLD-RTR data sets. Radio Sci 46:RS0C04. doi:10.1029/2011RS004683

5. Jin SG, Komjathy A (2010) GNSS reflectometry and remote sensing: new objectives and results. Adv Space Res 46(2):111–117. doi:10.1016/j.asr.2010.01.014
6. Marchán-Hernández JF, Camps A, Rodríguez-Álvarez N et al (2009) An efficient algorithm to the simulation of delay–Doppler maps of reflected global navigation satellite system signals. IEEE Trans Geosci Remote Sens 47(8):2733–2740
7. Valencia E, Camps A, Rodriguez-Alvarez N et al (2013) Using GNSS-R imaging of the ocean surface for oil slick detection. IEEE J Sel Top Appl Earth Obs Remote Sens 6(1):217–223
8. Masters D, Axelrad P, Katzberg S (2004) Initial results of land-reflected GPS bistatic radar soil moisture measurements in SMEX02. Remote Sens Environ 92:507–520
9. Liang P, Pierce LE, Moghaddam M (2005) Radiative transfer model for microwave bistatic scattering from forest canopies. IEEE Trans Geosci Remote Sens 43:2470–2483
10. Ulaby FT, Sarabandi K, McDonald K et al (1990) Michigan microwave canopy scattering model. Int J Remote Sens 11:1223–1253
11. Ulaby FT, Elachi C (1990) Radar polarimetry for geoscience applications. Artech House Publishers, Norwood, MA, USA
12. Ferrazzoli P, Guerriero L, Pierdicca N et al (2010) Forest biomass monitoring with GNSS-R: theoretical simulations. Adv Space Res doi:10.1016/j.asr.2010.04.02